Available online at www.sciencedirect.com
ScienceDirect
Journal of Solid State Chemistry 180 (2007) 2305–2309
JOURNAL OF SOLID STATE CHEMISTRY
www.elsevier.com/locate/jssc

Crystal structure and structural disorder of $(Ba_{0.65}Ca_{0.35})_2SiO_4$

Koichiro Fukuda*, Masamichi Ito, Tomoyuki Iwata

Department of Environmental and Materials Engineering, Nagoya Institute of Technology, Nagoya 466-8555, Japan

Received 16 March 2007; received in revised form 25 May 2007; accepted 2 June 2007
Available online 8 June 2007

Abstract

Crystal structure and structural disorder of $(Ba_{0.65}Ca_{0.35})_2SiO_4$ were investigated by laboratory X-ray powder diffraction ($CuK\alpha_1$). The initial structural model with eleven independent atoms in the unit cell was determined using direct methods, and it was further modified to a split-atom model, in which the two types of Ba/Ca atoms and two types of SiO_4 tetrahedra were, respectively, positionally and orientationally disordered. The crystal structure is trigonal (space group $P\bar{3}m1$, $Z=4$) with lattice dimensions $a=0.57505(1)$ nm, $c=1.46706(2)$ nm and $V=0.42014(1)$ nm^3. The validity of the structural model was verified by the three-dimensional electron density distribution, the structural bias of which was reduced as much as possible using the maximum-entropy methods-based pattern fitting (MPF). The final reliability indices calculated from the MPF were $R_{wp}=9.56\%$ ($S=1.48$), $R_p=7.29\%$, $R_B=1.82\%$ and $R_F=0.88\%$. This compound is most probably homeotypic to glaserite.

Keywords: Barium calcium silicate; X-ray powder diffraction; Direct methods; Rietveld method; Maximum entropy method; Electron density distribution; Disordered structure

1. Introduction

Phase stability in the binary system Ba_2SiO_4–Ca_2SiO_4 has been extensively studied because of its importance in cement chemistry as well as in silicate mineralogy [1–4]. In the region of $(Ba_{0.6}Ca_{0.4})_2SiO_4$–$(Ba_{0.775}Ca_{0.225})_2SiO_4$, Brisi [1] has found a new phase and termed it phase *T*. Later this compound was examined by X-ray power diffraction (XRPD) and electron-beam diffraction to demonstrate the hexagonal unit cell of *a* and 2*c*, where *a* and *c* correspond to the unit cell of α-Ca_2SiO_4 [2,3]. The Laue class has been determined to be $\bar{3}m$ (trigonal) by single-crystal X-ray diffraction (Laue and precession) methods [4], however, the crystal structure is still not elucidated so far.

The polymorphic modifications of Ca_2SiO_4 established so far are, at ordinary pressures, γ, α'_L, α'_H and α in order of increasing temperature [5]. The β phase, stable at high pressures, occurs metastably on rapid cooling. The crystal structure of the γ phase is similar to that of olivine. On the other hand, the crystal structure of Ba_2SiO_4 [6] and those of the α'_L, α'_H α and β polymorphs all belong to a large family typified by that of glaserite, $K_3Na(SO_4)_2$ (space group $P\bar{3}m1$ with lattice dimensions $a=0.56801$ nm and $c=0.7309$ nm) [7].

Recent advances in the field of crystal-structure analysis from XRPD data have enabled us to investigate complex structures, including positional disordering of atoms and orientational disordering of atomic groups. The initial structural models may be determined by, for example, direct methods [8]. The structural parameters are subsequently refined using the Rietveld method [9]. In order to disclose the structural details that had not been introduced into the structural models, the combined use of a maximum-entropy method (MEM) [10] and a MEM-based pattern fitting (MPF) method [11] is employed. The Rietveld and MEM analyses are insufficient to readily determine a charge density because the observed structure factors, F_o (Rietveld), are biased toward the structural model. The subsequent MPF method reduces the bias as much as possible. Thus, the MEM and MPF analyses are

*Corresponding author. Fax: +81 52 735 5289.
E-mail address: fukuda.koichiro@nitech.ac.jp (K. Fukuda).

0022-4596/$ - see front matter © 2007 Elsevier Inc. All rights reserved.
doi:10.1016/j.jssc.2007.06.001

alternately repeated (REMEDY cycle) until the reliability indices no longer decrease. Crystal structures are represented not by structural parameters but by electron densities in MPF.

In the present study, we have for the first time determined the crystal structure of the T phase. The initial structural model was derived from XRPD data by direct methods, and it was further modified to a split-atom model. The electron density distribution (EDD) determined by MPF was satisfactorily expressed by the split-atom model.

2. Experimental

2.1. Synthesis

A specimen of $(Ba_{0.65}Ca_{0.35})_2SiO_4$ was prepared from stoichiometric amounts of reagent-grade chemicals $BaCO_3$, $CaCO_3$ and SiO_2. Well-mixed chemicals were pressed into pellets (12 mm diameter and 3 mm thick), heated at 1773 K for 5 h, followed by quenching in air.

2.2. Characterization

X-ray powder diffraction intensities were collected at 298 K on a PANalytical X'Pert PRO Alpha-1 diffractometer equipped with a high-speed detector (X'Celerator) in Bragg-Brentano geometry in a 2θ range from 17.0032° to 148.4958° using monochromatized Cu$K\alpha_1$ radiation (45 kV, 40 mA). The divergence slit of 0.5° was employed to collect the quantitative profile intensities over the whole 2θ range. Other experimental conditions were: continuous scan, total of 15,738 datapoints and total experimental time of 24.5 h. The positional parameters of atoms were standardized using the computer program STRUCTURE TIDY [12]. The three-dimensional EDD and crystal-structure models were visualized using the software package VENUS [13].

3. Results and discussion

3.1. Initial structural model

Peak positions of the experimental diffraction pattern were first determined using the computer program PowderX [14]. The 2θ values of 25 observed peak positions were then used as input data to the automatic indexing computer program TREOR90 [15]. One hexagonal unit cell was found with satisfactory figures of merit: $M20/F20 = 27/19$ (0.017645, 60) and $M25/F25 = 24/19$ (0.017480, 77) [16,17]. The derived unit-cell parameters of $a = 0.57554(5)$ nm and $c = 1.4686(1)$ nm, which is comparable to those determined in previous studies [2,4], could index all reflections, including weak ones, in the experimental diffraction pattern.

The integrated intensities were refined by the whole powder-pattern decomposition method, based on the Pawley algorithm [18], using the computer program WPPF [19]. The observed diffraction peaks were examined to confirm the presence or absence of reflections. No systematic absences for $h\,k\,i\,l$ reflections were found, which implies that the possible space groups belonging to the Laue class $\bar{3}m$ are $P321$, $P3m1$, $P\bar{3}m1$, $P312$, $P31m$ and $P\bar{3}1m$. All of the possible space groups were tested using the EXPO2004 package [8] for the search of a crystal-structure model. A promising structural model with a minimum reliability index R_F [20] of 15.1% was obtained with the space group $P\bar{3}m1$ in a default run of the program. This space group is one of the most probable ones that were proposed in a previous study [4]. There were eleven independent sites in the unit cell; five Ba/Ca sites of Wyckoff positions 2d (denoted by $M1$), 1a ($M2$), 2d ($M3$), 2c ($M4$) and 1b ($M5$), two Si sites of 2d (Si1 and Si2) and four O sites of 6i (O1), 2d (O2), 6i (O3) and 2d (O4). The derived crystal structure is very similar to that of glaserite [7], although the c-axis length of the former is about twice as long as that of the latter.

Structural parameters of all atoms were refined by the Rietveld method using the computer program RIETAN-FP [21]. A Legendre polynomial was fitted to background intensities with twelve adjustable parameters. The split pseudo-Voigt function [22] was used to fit the peak profile. In the initial stage of the refinement process, the occupancies of Ba and Ca atoms in each Ba/Ca site were fixed at 65% and 35%, respectively. The individual occupancies were finally refined under the constraints that the total number of Ba atoms on these sites and that of Ca atoms were unchanged. Because the site occupancies and the corresponding isotropic displacement (B) parameters were strongly correlated, they were refined alternately in successive least-squares cycles. The refinement resulted in the relatively large B parameters for $M1$, $M2$, O1, O2 and O3 sites ($B(M1) = 1.73(9) \times 10^{-2}$ nm^2, $B(M2) = 7.1(3) \times 10^{-2}$ nm^2, $B(O1) = 6.3(3) \times 10^{-2}$ nm^2, $B(O2) = 11.2(10) \times 10^{-2}$ nm^2 and $B(O3) = 1.7(2) \times 10^{-2}$ nm^2) with the less satisfactory reliability (R) indices [20] of $R_{wp} = 11.19\%$ ($S = 1.74$), $R_p = 8.66\%$, $R_B = 3.97\%$ and $R_F = 2.00\%$.

The MPF method was subsequently applied, so as to extract structural details that had not been introduced into the structural model and consequently improve the EDD. After two REMEDY cycles, R_B and R_F decreased to 2.76% and 1.28%, respectively. The significant improvements of these R factors indicate that the crystal structure is represented more adequately with electron densities than with the structural model. The EDD at the $M1$, $M2$, O1, O2 and O3 sites showed broadening, which would correspond to the large B parameters. For example, the two-dimensional map in the region of $0.54 \leqslant z \leqslant 0.55$ clearly demonstrates that the oxygen atoms at O2 site are split to occupy the three sites around the rotation triad axis (Fig. 1). On the other hand, the EDD at the $M3$, $M4$, $M5$, Si1, Si2 and O4 sites were in accord with the atomic positions of the initial model. These findings promoted us to build split-atom models for $M1$, $M2$, O1, O2 and O3 sites.

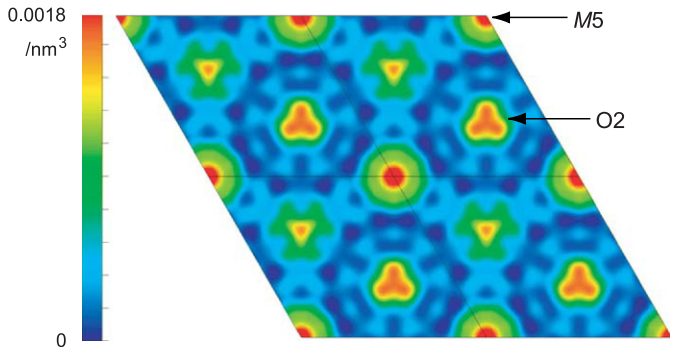

Fig. 1. Electron density distribution determined by MPF method with the initial structural model. Two-dimensional map parallel to (001) at $z = 0.54$.

Table 1
Crystal data for $(Ba_{0.65}Ca_{0.35})_2SiO_4$

Chemical composition	$(Ba_{0.65}Ca_{0.35})_2SiO_4$
Space group	$P\bar{3}m1$
a/nm	0.57505(1)
c/nm	1.46706(2)
V/nm^3	0.42014(1)
Z	4
D_x/Mgm^{-3}	4.72

Table 2
Structural parameters for $(Ba_{0.65}Ca_{0.35})_2SiO_4$

Site	Wyckoff position	g	x	y	z	$100 \times B$/nm^2
$M1$	6i	1/3	0.654(1)	$-x$	0.1600(2)	0.64(9)
$M2$	6g	1/6	0.0854(7)	0	0	0.1(1)
$M3$	2d	1	1/3	2/3	0.3438(1)	0.11(3)
$M4$	2c	1	0	0	0.2439(4)	0.68(9)
$M5$	1b	1	0	0	1/2	0.18(4)
Si1	2d	1	1/3	2/3	0.1186(4)	0.7(1)
Si2	2d	1	1/3	2/3	0.6099(5)	0.7(1)
O1	12j	1/2	0.145(2)	0.360(2)	0.1595(8)	1.2(3)
O2	6i	1/3	0.715(2)	$-x$	0.496(1)	1.8(6)
O31	6i	1/2	0.812(2)	$-x$	0.336(1)	0.3(2)
O32	6i	1/2	0.828(1)	$-x$	0.370(1)	0.3
O4	2d	1	1/3	2/3	0.006(1)	0.8(2)

Site occupancies: $M1$: 65.7% Ba and 34.3% Ca; $M2$: 85.2% Ba and 14.8% Ca; $M3$: 99.2% Ba and 0.8% Ca; $M4$: 2.4% Ba and 97.6% Ca; $M5$: 100% Ba.

3.2. Split-atom model

The splitting of atoms was performed in two different ways; one was to decrease the site symmetry and the other was to split each site into two fractions. The point symmetry was decreased from $3m$ (Wyckoff position 2d) to m (6i) for both $M1$ and O2 sites, $\bar{3}m$ (1a) to 2 (6g) for $M2$ site, and m (6i) to 1 (12j) for O1 site, while the O3 site (6i) was split into two fractions. The Rietveld refinement with this split-atom model gave the lower reliability indices of $R_{wp} = 9.64\%$ ($S = 1.50$), $R_p = 7.33\%$, $R_B = 3.19\%$ and $R_F = 1.44\%$ as compared with the former Rietveld analysis. The crystal data are given in Table 1, and the final positional and B parameters of atoms are given in Table 2. The $M5$ sites were occupied by only Ba atoms, while the other Ba/Ca sites were statistically occupied by both Ba and Ca atoms.

Fig. 2 shows the perspective view of the crystal structure of $(Ba_{0.65}Ca_{0.35})_2SiO_4$. The $M1$ and O2 sites are displaced from their average positions to separate into three sites around the rotation triad axis. The $M2$ sites are split into six positions, forming doughnut-shaped six-membered rings. Each of these positions are on the rotation diad axes parallel to $\langle 100 \rangle$ or $\langle 110 \rangle$, which are related by sixfold rotation around the inversion triad axis. The O1 sites are detached from the {110} reflection planes to split into two general positions.

Because all the O atoms, including those showing positional disorder, must be rigidly bonded to Si atoms in the crystal structure, each SiO_4 tetrahedron is as a whole orientationally disordered. With $Si2O_4$ tetrahedra, the Si2–O2 directions make angles of 17.2° with the rotation triad axis passing through the Si2 site. These values are almost comparable to the O31–Si2–O32 angles of 18.3°. Accordingly, the disordered $Si2O_4$ tetrahedra can be regarded as a statistical average of the three different orientational configurations that are related by the triad axis. On the other hand, the disordered $Si1O_4$ tetrahedra can be regarded as a statistical average of the two configurations that are related by the {110} reflection planes. In Table 3, we reported only Si–O bonds and O–Si–O angles of SiO_4 tetrahedra belonging to one of the multiple orientations,

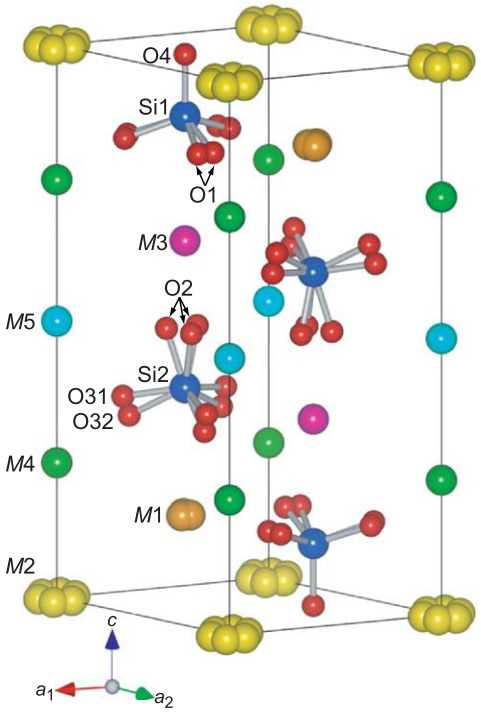

Fig. 2. Crystal structure of $(Ba_{0.65}Ca_{0.35})_2SiO_4$. Numbering of atoms corresponds to that given in Table 2.

excluding the bonds and angles between atoms of different orientation states. The mean bond lengths are in accord with the interatomic distance of 0.164 nm that is calculated from the ionic radii of Si^{4+} and O^{2-} in the fourfold coordination [$r(Si^{4+}) = 0.026$ nm and $r(O^{2-}) = 0.138$ nm] [23]. The mean values of the O–Si–O angles are almost 109°. These distances and angles are in good agreement with those found in other silicates [24].

The MPF method was subsequently applied in order to confirm the validity of the split-atom model. After two REMEDY cycles, R_{wp} (S), R_p, R_B and R_F decreased to 9.56% (1.48), 7.29%, 1.82% and 0.88%, respectively. Subtle changes in EDD arose out of MPF, which effectively improved the R_B and R_F factors. Observed, calculated, and difference XRPD patterns for the final MPF are plotted in Fig. 3. The three-dimensional EDD at the *M*2 sites has doughnut-shaped structure (Fig. 4). The corresponding two-dimensional map (Fig. 5(a)) clearly demonstrates that the electron density at the original position (1*a* site) is present in mere trace amounts. The two-dimensional map on (001) at the O2 sites (Fig. 5(b)) shows the three sharp maximum around the rotation triad axes. The EDD at the *M*1, O1, O31 and O32 sites (Fig. 4) show broadening, the equidensity isosurfaces of which are in fair agreement with the atom arrangements in Fig. 2. As a result, the EDD determined by MPF is explained satisfactorily by the present split-atom model. We therefore

Table 3
Si–O bond lengths (nm) and O–Si–O angles (deg.) in $(Ba_{0.65}Ca_{0.35})_2SiO_4$

Si1–O1	0.165(1) × 3
Si1–O4	0.165(1)
⟨Si1–O⟩	0.165
O1–Si1–O1	107.7(5) × 3
O1–Si1–O4	111.2(4) × 3
⟨O–Si1–O⟩	109.4
Si2–O2	0.163(2)
Si2–O31	0.164(1) × 2
Si2–O32	0.165(2)
⟨Si2–O⟩	0.164
O2–Si2–O31	108.7(7) × 2
O2–Si2–O32	101.6(10)
O31–Si2–O31	116.7(4)
O31–Si2–O32	110.0(5) × 2
⟨O–Si2–O⟩	109.3

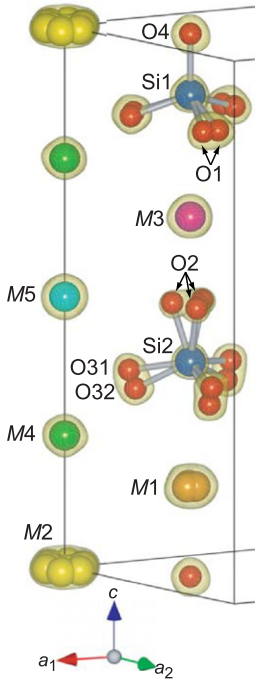

Fig. 4. Three-dimensional electron density distribution determined by MPF with the split-atom model. Isosurfaces expressed in wireframe style for an equidensity level of 0.0025 nm^{-3}.

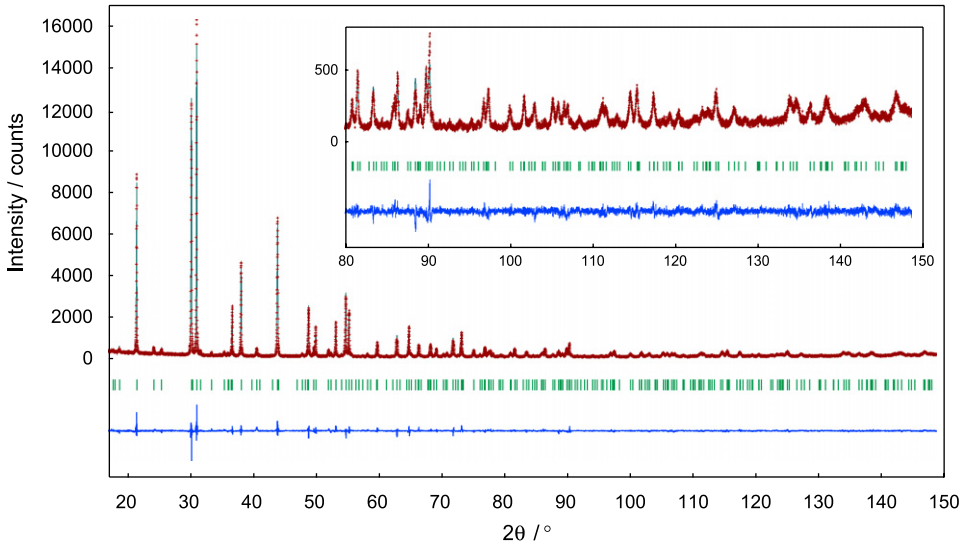

Fig. 3. Comparison of the observed diffraction pattern of $(Ba_{0.65}Ca_{0.35})_2SiO_4$ (symbol: +) with the corresponding calculated pattern (upper solid line). The difference curve is shown in the lower part of the diagram. Vertical bars indicate the positions of Bragg reflections.

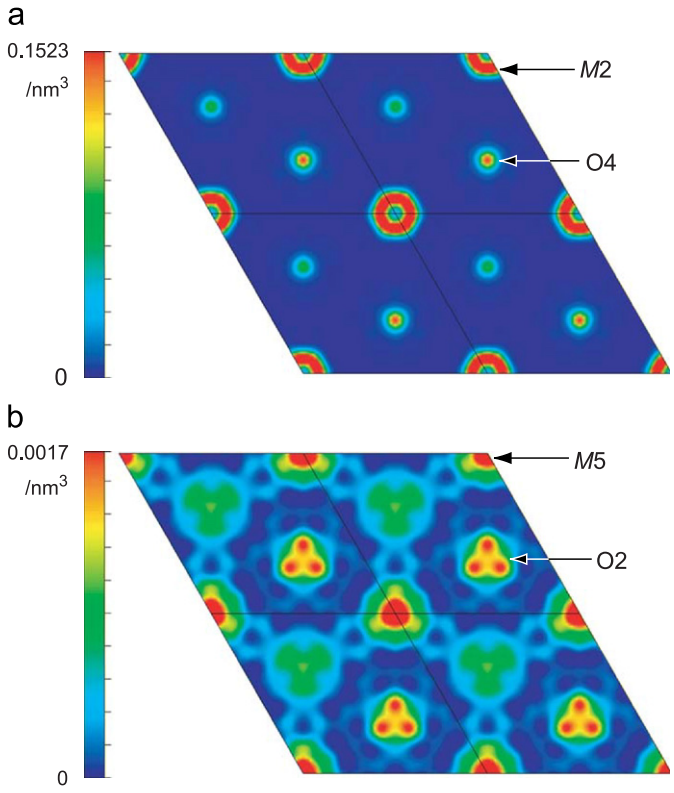

Fig. 5. Two-dimensional electron density distribution maps parallel to (001) in the regions of: (a) $0 \leqslant z \leqslant 0.03$ and (b) $0.53 \leqslant z \leqslant 0.55$. The *M*2 sites show doughnut-shaped rings in (a). The O2 sites demonstrate the three sharp maximum around the triad axis in (b).

concluded that, as long as the crystal structure was expressed by a structural model, the present split-atom model would be satisfactory. This compound is most probably homeotypic to glaserite.

4. Conclusion

The highly disordered crystal structure of the *T* phase in the system Ba_2SiO_4–Ca_2SiO_4 was successfully determined from XRPD data. The structure was expressed by the split-atom model, in which the two types of Ba/Ca atoms and two types of SiO_4 tetrahedra were, respectively, positionally and orientationally disordered. The three-dimensional EDD was finally determined by the MPF method, which was satisfactorily expressed by the present split-atom model.

Appendix A. Supplementary data

Supplementary data associated with this article can be found in the online version at doi:10.1016/j.jssc.2007.06.001.

References

[1] C. Brisi, Cesare. Ind. Ital. Cem. 33 (1963) 397–402.
[2] B. Matkovic, S. Popovic, B. Grzeta, J. Am. Ceram. Soc. 69 (1986) 132–134.
[3] J.G. Thompson, R.L. Withers, B.G. Hyde, J. Am. Ceram. Soc. 70 (1987) 383–386.
[4] K. Fukuda, I. Maki, K. Adachi, J. Am. Ceram. Soc. 75 (1992) 884–888.
[5] H.F.W. Taylor, Cement Chemistry, Thomas Telford Publishing, London, UK, 1997, pp. 1–28.
[6] H.P. Grosse, E. Tillmanns, Cryst. Struct. Commun. 3 (1974) 599–602.
[7] K. Okada, J. Ossaka, Acta Crystallogr. B 36 (1980) 919–921.
[8] A. Altomare, M.C. Burla, M. Camalli, B. Carrozzini, G.L. Cascarano, C. Giacovazzo, A. Guagliardi, A.G.G. Moliterni, G. Polidori, R. Rizzi, J. Appl. Crystallogr. 32 (1999) 339–340.
[9] H.M. Rietveld, J. Appl. Crystallogr. 2 (1969) 65–71.
[10] M. Takata, E. Nishibori, M. Sakata, Z. Kristallogr. 216 (2001) 71–86.
[11] F. Izumi, S. Kumazawa, T. Ikeda, W.-Z. Hu, A. Yamamoto, K. Oikawa, Mater. Sci. Forum 378–381 (2001) 59–64.
[12] L.M. Gelato, E. Parthé, J. Appl. Crystallogr. 20 (1987) 139–143.
[13] F. Izumi, R.A. Dilanian, Commission on powder diffraction, IUCr Newslett. 32 (2005) 59–63.
[14] C. Dong, J. Appl. Crystallogr. 32 (1999) 838.
[15] P.E. Werner, L. Eriksson, M. Westdahl, J. Appl. Crystallogr. 18 (1985) 367–370.
[16] P.M. de Wolff, J. Appl. Crystallogr. 1 (1968) 108–113.
[17] G.S. Smith, R.L. Snyder, J. Appl. Crystallogr. 12 (1979) 60–65.
[18] G.S. Pawley, J. Appl. Crystallogr. 14 (1981) 357–361.
[19] H. Toraya, J. Appl. Crystallogr. 19 (1986) 440–447.
[20] R.A. Young (Ed.), The Rietveld Method, Oxford University Press, Oxford, UK, 1993, pp. 1–38.
[21] F. Izumi, T. Ikeda, Mater. Sci. Forum 321–324 (2000) 198–203.
[22] H. Toraya, J. Appl. Crystallogr. 23 (1990) 485–491.
[23] R.D. Shannon, Acta Crystallogr. A 32 (1976) 751–767.
[24] W.H. Baur, Am. Mineral. 56 (1971) 1573–1599.